

# Mathematical Model of Enzyme Clustering in Glucose Metabolism for Cancer Treatment

## 1. Problem Statement

Interpreting scientific papers is a challenging but essential skill in biomedical engineering. To strengthen this ability, I analyzed “*A Mathematical Model for Enzyme Clustering in Glucose Metabolism*” by Miji Jeon. This paper, which applies mathematical modeling to a biological process I find particularly interesting, serves as the foundation for the discussion in this section. (Full reference provided at the end.)

Cancer cells reprogram their metabolism to prioritize growth. This is often done by altering enzyme functions and forming clusters called glucosomes to redirect glucose metabolism to different metabolic pathways. The three metabolic pathways in this instance are glycolysis, pentose phosphate pathway, and serine biosynthesis. This study investigates how these clusters affect these key metabolic pathways by creating a mathematical model. The experiment aims to understand how changes in cluster size and enzyme activity influence cancer metabolism. If a pathway experiences an increase in activity, we can determine cancer cells rely more on those biochemical reactions. If a pathway experiences a decrease in activity, it indicates a loss of normal cellular function that can be exploited in combating cancer and potentially revealing new targets for therapy.

## Approach to Solve the Problem

We construct a mathematical model using ODEs to describe the glycolytic and gluconeogenic pathways. This includes:

- 7 metabolic intermediates (S)
- 9 enzyme-associated species (E)

- 3 metabolic products (P)
- 28 propensity reactions (R)

The focus is on the enzymes that form the multienzyme complex, which include PFKL, FBPase, PKM2, and PEPCK1. These enzymes are believed to exhibit cluster behavior in their activity depending on their size. To measure the direction of glucose flux, we plot the metabolic products P1, P2, and P3, which represent metabolic outcomes.

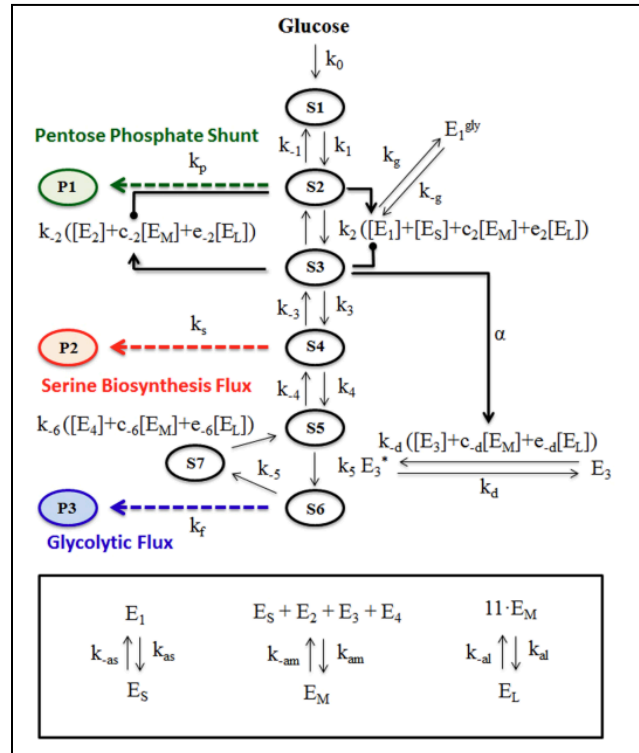


Figure 1: Simplified glucose metabolism with multienzyme complexes

## Metabolic Pathways

**Glycolysis:** This is the process your cells use to break down sugar (like glucose) into smaller pieces mainly producing energy. We can think of it like a machine breaking down a big block of sugar into smaller chunks, and during this process, the cell gets energy in the form of ATP to fuel other activities.

**Pentose Phosphate:** This pathway also starts with glucose, but instead of just breaking it down for energy, it creates important molecules that help the cell grow and repair itself. The Pentose Phosphate Pathway is especially important for cells that are dividing quickly such as cancer cells.

Biosynthesis: This pathway involves the creation of serine, an amino acid (building block of proteins), which is used in many important processes like making proteins, growing cells, and maintaining the cell's structure. We can think of it as a small factory inside the cell that produces an essential ingredient needed for building the cell and its functions.

It is important to keep in mind the key question we are asking ourselves: How does enzyme cluster size impact metabolic pathway flux?

## 2. Structure and Functional Basis

Enzyme Activity and Cluster Size: The enzyme activities are modeled to vary depending on the size of the glucosome clusters.

- Small clusters are assumed to exhibit standard enzyme activity.
- Medium/large clusters are assumed to alter the glucose flux into different metabolic pathways. Medium clusters promote the diversion of glucose to the pentose phosphate pathway, while large clusters drive glucose toward biosynthesis.

Differential Equations and Enzyme Kinetics: The model uses differential equations to simulate the dynamics of glucose flux and its regulation through the allosteric control of enzymes. These enzymes exhibit Michaelis-Menten kinetics. Michaelis-Menten kinetics is a model that describes how enzyme reaction rates depend on substrate concentration. Reaction rates depend on the concentration of substrates and the enzymes' allosteric regulation by metabolites. Parameters for enzyme activities in different cluster sizes are adjusted to reflect the changing metabolic needs of cancer cells.

## 3. Experiment

### Validation

Dimension Check: For this particular model, all parameters are

non-dimensional.

Numerical Check: Parameters in the model are verified to be consistent with the qualitative changes in glucose flux in popular scientific literature.

Experiment Validation: To validate the model, experimental methods involving cell culture and imaging were used. This allows for the visualization of glucosome clusters in live cells. The experimental results can be compared to our model's predictions to assess the accuracy and reliability of the proposed mathematical framework.

Variables	Chemical species	Values (non-dimensional)
$S_1(0)$	Glucose	0.01
$S_2(0)$	Fructose-6-Phosphate	0.01
$S_3(0)$	Fructose-1,6-Bisphosphate	0.01
$S_4(0)$	3-Phosphoglycerate	0.01
$S_5(0)$	Phosphoenolpyruvate	0.01
$S_6(0)$	Pyruvate	0.01
$S_7(0)$	Oxaloacetate	0.01
$E_1(0)$	Phosphofructokinase 1	99.99
$E_2(0)$	Fructose-1,6-Bisphosphatase	100
$E_3(0)$	Pyruvate Kinase M2 dimers	99.99
$E_4(0)$	Phosphoenolpyruvate Carboxykinase 1	100
$E_S(0)$	Small-sized enzyme clusters	0
$E_M(0)$	Medium-sized enzyme clusters	0
$E_L(0)$	Large-sized enzyme clusters	0
$E_3^*(0)$	Pyruvate Kinase M2 tetramers	0.01
$E_1^{gly}(0)$	Glycosylated Phosphofructokinase	0.01
$P_1(0)$	Pentose Phosphate Shunt	0.01
$P_2(0)$	Serine Biosynthesis Flux	0.01
$P_3(0)$	Glycolytic Flux	0.01

*Figure 2: The initial conditions used in the mathematical model for the glucose metabolic pathway*

Parameters	Rates	Values (non-dimensional)
$k_0$	Glucose production	10
$k_1, k_{-1}$	Conversion to (from) Fructose-6-Phosphate	10, 10
$k_2, k_{-2}$	Conversion to (from) Fructose-1,6-Bisphosphate	40, 7
$k_3, k_{-3}$	Conversion to (from) 3-Phosphoglycerate	10, 10
$k_4, k_{-4}$	Conversion to (from) Phosphoenolpyruvate	14, 7
$k_5$	Conversion to Pyruvate	1
$k_{-5}$	Conversion to Oxaloacetate	10
$k_{-6}$	Conversion to Phosphoenolpyruvate from Oxaloacetate	10
$k_{as}, k_{-as}$	Small enzyme cluster association/disassociation	10, 10
$k_{am}, k_{-am}$	Medium enzyme cluster association/disassociation	10, 10
$k_{al}, k_{-al}$	Large enzyme cluster association/disassociation	10, 10
$k_g, k_{-g}$	Phosphofructokinase glycosylation (de-glycosylation)	1, 1
$k_{d1}, k_{-d1}$	Conversion of Pyruvate Kinase M2 from (to) tetramer to (from) dimer	1, 1
$k_p$	Pentose Phosphate Shunt	5
$k_s$	Serine Biosynthesis Shunt	5
$k_f$	Glycolytic Flux	5
$\delta_p$	Degradation of the Pentose Phosphate Flux	0.5
$\delta_s$	Degradation of Serine Biosynthesis Flux	0.5
$\delta_f$	Degradation of Glycolytic Flux	0.5
$c_2$	Activation of conversion to Fructose-1,6-Bisphosphate by medium enzyme clusters	0.2
$c_{-2}$	Activation of conversion from Fructose-1,6-Bisphosphate by medium enzyme clusters	10
$c_{-6}$	Activation of conversion to Phosphoenolpyruvate from Oxaloacetate by medium enzyme clusters	10
$c_{-d}$	Activation of conversion from Pyruvate Kinase M2 dimers to Pyruvate Kinase M2 tetramers by medium enzyme clusters	0.1
$e_2$	Activation of conversion to Fructose-1,6-Bisphosphate by large enzyme clusters	2.5
$e_{-2}$	Activation of conversion from Fructose-1,6-Bisphosphate by large enzyme clusters	0.1
$e_{-6}$	Activation of conversion to Phosphoenolpyruvate from Oxaloacetate by large enzyme clusters	10
$e_{-d}$	Activation of conversion from Pyruvate Kinase M2 dimers to Pyruvate Kinase M2 tetramers by large enzyme clusters	0.05
$\alpha$	Acceleration of Fructose-1,6-Bisphosphate on Pyruvate Kinase M2 association	1
$K_1$	Allosteric inhibition by Fructose-1,6-Bisphosphate	1
$K_2$	Allosteric inhibition by Fructose-6-Phosphate	1
$K_3$	Allosteric activation by Fructose-1,6-Bisphosphate	1

Figure 3: The rate constants used in the mathematical model for the glucose metabolic pathway

Reaction	Propensity	Reaction	Propensity	Reaction	Propensity
$R_1$	$k_0$	$R_{11}$	$k_{-5}S_6$	$R_{21}$	$k_dE_3^*$
$R_2$	$k_1S_1$	$R_{12}$	$k_{-6}(E_4 + c_{-6}E_M + e_{-6}E_L)S_7$	$R_{22}$	$k_{-d}(E_3 + c_{-d}E_M + e_{-d}E_L)(1 + \alpha(S_3)/(S_3 + K_3))$
$R_3$	$k_{-1}S_2$	$R_{13}$	$k_{as}E_1$	$R_{23}$	$k_pS_2$
$R_4$	$k_2(E_1 + E_5 + c_2E_M + e_2E_L)S_2(K_1)/(K_1 + S_3)$	$R_{14}$	$k_{-as}E_5$	$R_{24}$	$k_sS_4$
$R_5$	$k_{-2}(E_2 + c_{-2}E_M + e_{-2}E_L)S_3(K_2)/(K_2 + S_2)$	$R_{15}$	$k_{am}E_3E_2E_3E_4$	$R_{25}$	$k_fS_6$
$R_6$	$k_3S_3$	$R_{16}$	$k_{-am}E_M$	$R_{26}$	$\delta_pP_1$
$R_7$	$k_{-3}S_4$	$R_{17}$	$k_{al}(E_M)^{11}$	$R_{27}$	$\delta_sP_2$
$R_8$	$k_4S_4$	$R_{18}$	$k_{-al}E_L$	$R_{28}$	$\delta_fP_3$
$R_9$	$k_{-4}S_5$	$R_{19}$	$k_gE_1$		
$R_{10}$	$k_5E_3^*S_5$	$R_{20}$	$k_{-g}E_1^{gly}$		

Figure 4: Propensities of 28 reactions in the glucose metabolic pathway

Equations
$S = (S_1, S_2, S_3, S_4, S_5, S_6, S_7)^T, E = (E_1, E_2, E_3, E_4, E_5, E_M, E_L, E_3^*, E_1^{*by})^T, P = (P_1, P_2, P_3)^T$
$\frac{dS}{dt} = \nu_S \mathcal{R}_S(S, E), \frac{dE}{dt} = \nu_E \mathcal{R}_E(S, E), \frac{dP}{dt} = \nu_P \mathcal{R}_P(S, P)$
$\mathcal{R}_S(S, E) = [R_1, R_2, R_3, R_4, R_5, R_6, R_7, R_8, R_9, R_{10}, R_{11}, R_{12}, R_{23}, R_{24}, R_{25}]^T$ $\mathcal{R}_E(S, E) = [R_{13}, R_{14}, R_{15}, R_{16}, R_{17}, R_{18}, R_{19}, R_{20}, R_{21}, R_{22}]^T$ $\mathcal{R}_P(S, P) = [R_{23}, R_{24}, R_{25}, R_{26}, R_{27}, R_{28}]^T$
$\nu_S = \begin{bmatrix} 1 & -1 & 1 & 0 & 0 & 0 & 0 & 0 & 0 & 0 & 0 & 0 & 0 & 0 & 0 \\ 0 & 1 & -1 & -1 & 1 & 0 & 0 & 0 & 0 & 0 & 0 & 0 & -1 & 0 & 0 \\ 0 & 0 & 0 & 1 & -1 & -1 & 1 & 0 & 0 & 0 & 0 & 0 & 0 & 0 & 0 \\ 0 & 0 & 0 & 0 & 0 & 0 & 1 & -1 & -1 & 1 & 0 & 0 & 0 & -1 & 0 \\ 0 & 0 & 0 & 0 & 0 & 0 & 0 & 0 & 1 & -1 & -1 & 0 & 1 & 0 & 0 \\ 0 & 0 & 0 & 0 & 0 & 0 & 0 & 0 & 0 & 1 & -1 & 0 & 0 & 0 & -1 \\ 0 & 0 & 0 & 0 & 0 & 0 & 0 & 0 & 0 & 0 & 1 & -1 & 0 & 0 & 0 \end{bmatrix}$ $\nu_E = \begin{bmatrix} -1 & 1 & 0 & 0 & 0 & 0 & -1 & 1 & 0 & 0 \\ 0 & 0 & -1 & 1 & 0 & 0 & 0 & 0 & 0 & 0 \\ 0 & 0 & -1 & 1 & 0 & 0 & 0 & 0 & 1 & -1 \\ 0 & 0 & -1 & 1 & 0 & 0 & 0 & 0 & 0 & 0 \\ 1 & -1 & -1 & 1 & 0 & 0 & 0 & 0 & 0 & 0 \\ 0 & 0 & 1 & -1 & -11 & 11 & 0 & 0 & 0 & 0 \\ 0 & 0 & 0 & 0 & 1 & -1 & 0 & 0 & 0 & 0 \\ 0 & 0 & 0 & 0 & 0 & 0 & 0 & 0 & -1 & 1 \\ 0 & 0 & 0 & 0 & 0 & 0 & 1 & -1 & 0 & 0 \end{bmatrix}$ $\nu_P = \begin{bmatrix} 1 & 0 & 0 & -1 & 0 & 0 \\ 0 & 1 & 0 & 0 & -1 & 0 \\ 0 & 0 & 1 & 0 & 0 & -1 \end{bmatrix}$

Figure 5: System of differential equations to model enzyme clustering.

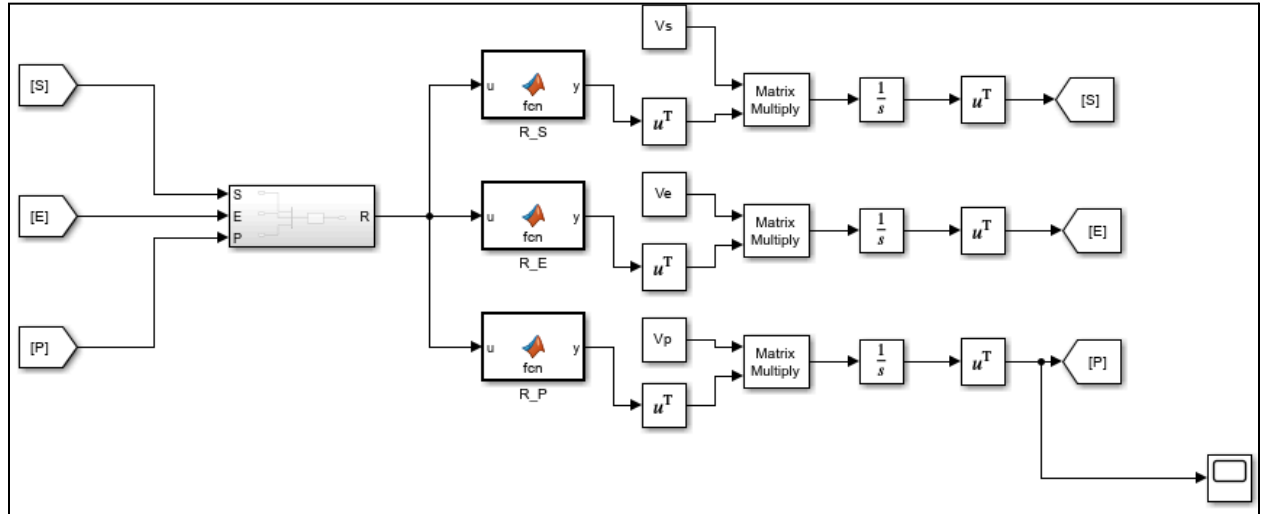


Figure 6: Mathematical model for enzyme clustering in glucose metabolism implemented in MATLAB/Simulink.

## 4.Results

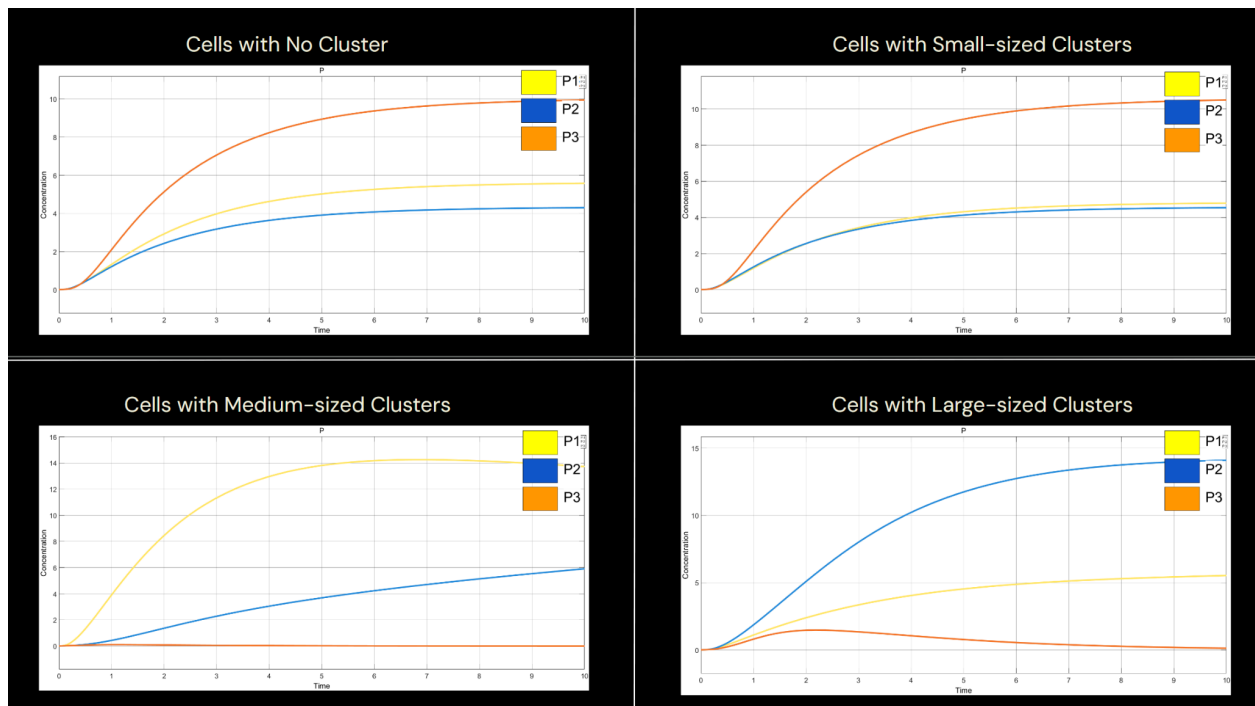


Figure 7: Simulation Results

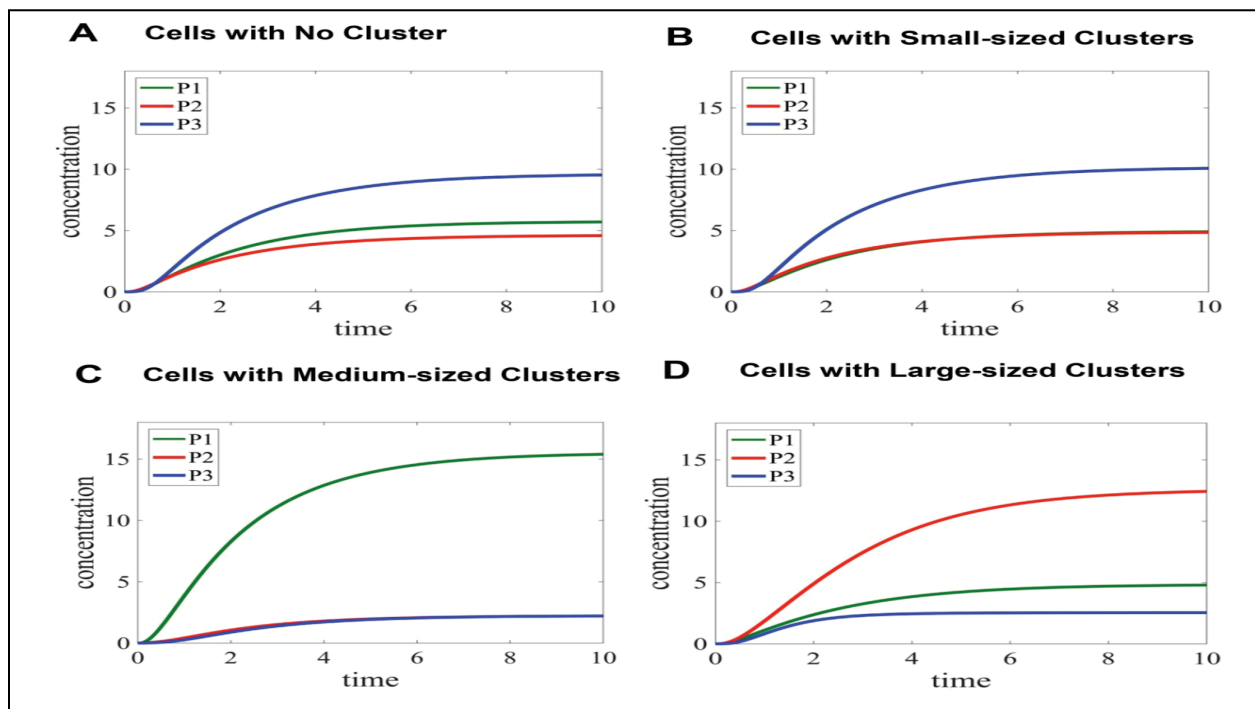


Figure 7: Original Experimental Results

## Explanation of Results

In the experiment, P1 is the pentose phosphate shunt, P2, is serine biosynthesis, and P3 is glycolysis. The simulation shows that the size of glucosome clusters does affect the direction of glucose flux. The simulation for no clusters and small-sized clusters showed the highest level of P3, which indicates that most of the glucose flux flows to glycolysis to produce pyruvate. The simulation for medium-sized clusters yielded a significant increase in P1 and a decrease in P2 and P3. Medium-sized clusters may have different levels of catalytic activity due to the increased flux of the pentose phosphate shunt. It is also correlated with high levels of medium-sized clusters in cancer cells, which may explain why our simulation yielded slightly different results compared to the original experiment. The simulation of large-sized clusters resulted in an increase in P2.

## 5. Discussion of Research Opportunities

Determining the correct treatment target is only half of the challenge. Acting on this knowledge requires the development and application of advanced biomedical technologies capable of translating theory into measurable clinical outcomes. Potential areas of research that extend from this problem space include biophotonics, neuroengineering, bioinstrumentation, and computational modeling of physiological systems. Each of these disciplines integrates core electrical and computer engineering principles with biology, offering distinct pathways to design technologies that acquire, process, and interpret complex biological signals.

I am particularly motivated by the prospect of contributing to this translation from mathematical models to practical tools. For example, biophotonics enables noninvasive probing of tissue structure and function using light, while neuroengineering applies circuit design and signal processing to study and interface with neural systems. Bioinstrumentation, on the other hand, offers the opportunity to design precise measurement and monitoring devices for use in clinical and research settings. These approaches, when combined with rigorous computational modeling, represent a powerful framework for addressing pressing biomedical challenges.



My long-term goal is to pursue graduate research at this intersection, developing methods and devices that not only provide fundamental insights into human physiology but also directly improve diagnosis, monitoring, and treatment. By advancing the engineering foundations of biomedical technology, I aim to contribute to solutions that have a tangible impact on patient care and global health outcomes.

## 6. Conclusion

I implemented a mathematical model to explore how cluster size and multienzyme complexes of metabolic enzymes contribute to cancer cell metabolism by altering glucose flux. Although I did not model the specific effects of 2-deoxyglucose (2-DG) since it was used experimentally, its role in disrupting glycolysis and redirecting glucose metabolism to other pathways is well-established in experimental studies. Ultimately, by analyzing how glucose flux changes in cancer cells, our model provides insights into potential metabolic vulnerabilities that could be exploited for treating cancers with high glycolytic activity like breast cancer

## 7. References

eon, Miji, et al. "A Mathematical Model for Enzyme Clustering in Glucose Metabolism." Scientific Reports, vol. 8, no. 1, 9 Feb. 2018,

Link: <https://doi.org/10.1038/s41598-018-20348-7>.